Supporting Information

Ultra-small Rh nanoparticles supported on WO_{3-x} nanowires as efficient catalysts for visible-light-enhanced hydrogen evolution from ammonia borane

*Xiao Li,[a] Yucong Yan,[a] Yi Jiang,[a] Xingqiao Wu,[a] Shi Li,[a] Jingbo Huang,[a] Junjie Li,[a] Yangfan Lin,[a] Deren Yang[a] and Hui Zhang[a,]**

[a]State Key Laboratory of Silicon Materials, School of Materials Science and Engineering, Zhejiang University, Hangzhou, Zhejiang 310027, People's Republic of China. Email: msezhanghui@zju.edu.cn

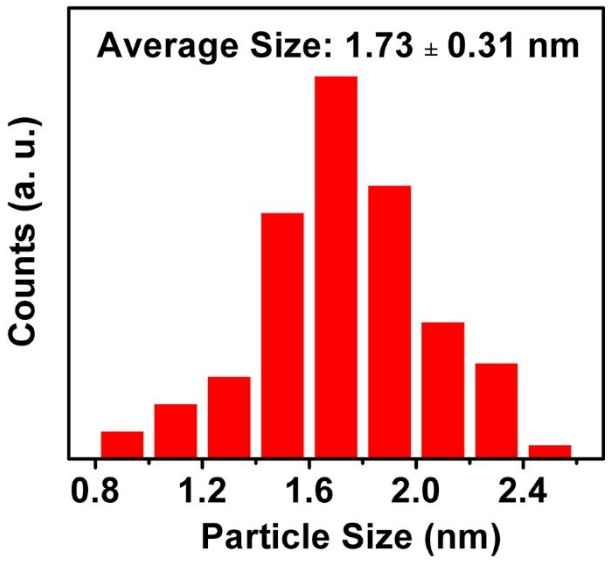

Fig S1. Size distribution of the Rh nanoparticles in the Rh/WO_{3-x}-2 hybrid nanowires.

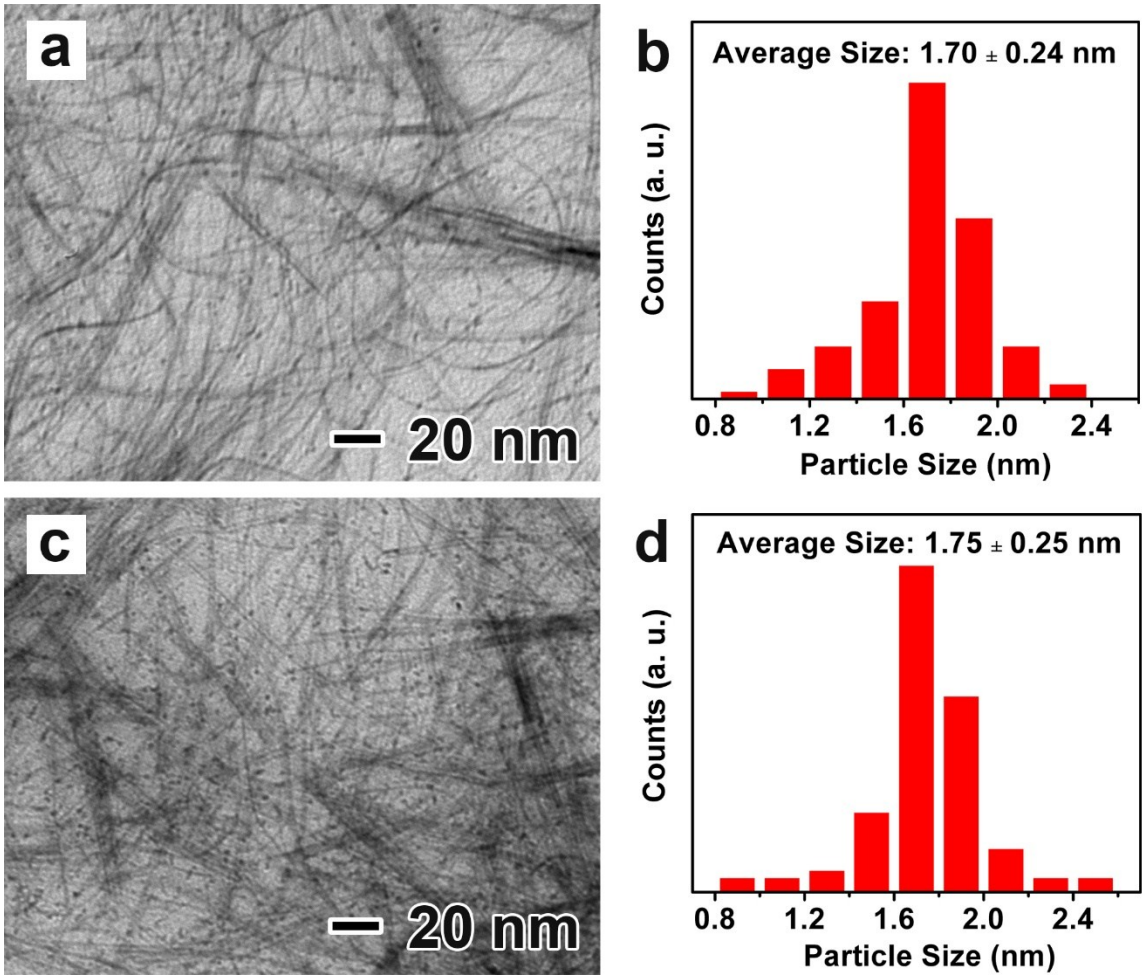

Fig S2. (a, c) TEM images and (b, d) corresponding size distributions for the Rh nanoparticles of Rh/WO_{3-x}-1 and Rh/WO_{3-x}-3 hybrid nanowires, respectively.

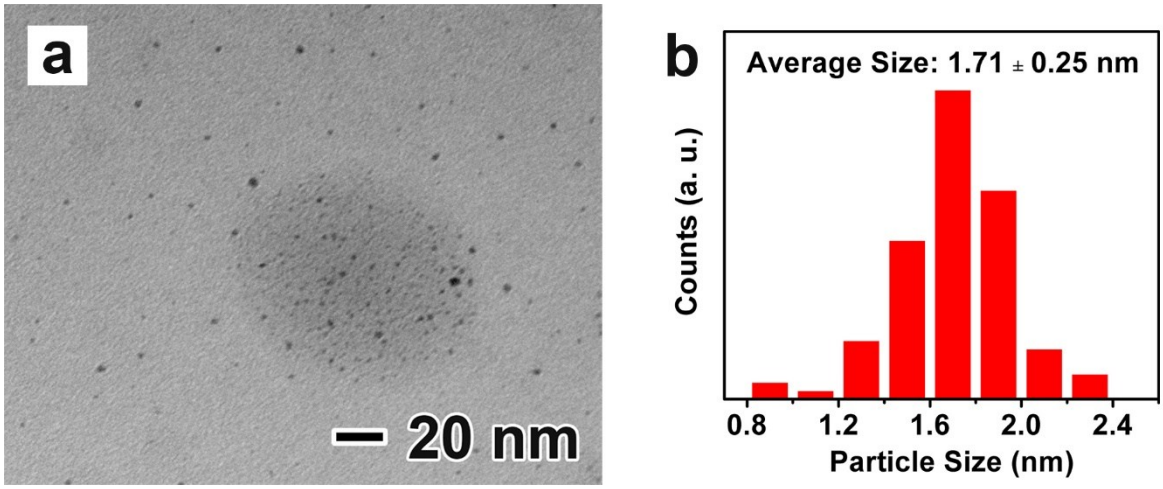

Fig S3. (a) TEM image and (b) corresponding size distribution of the Rh nanoparticles.

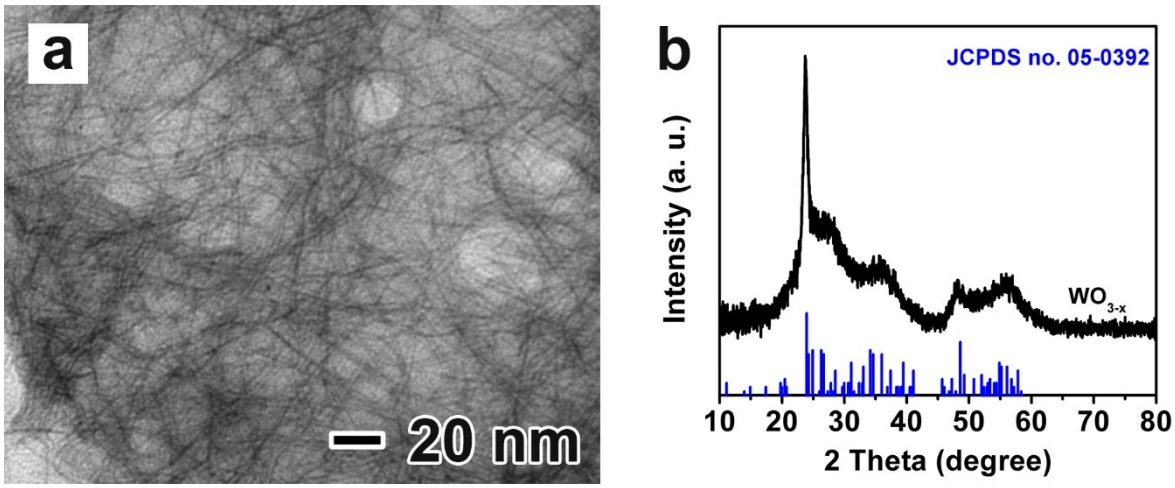

Fig S4. (a) TEM image and (b) XRD pattern of the WO_{3-x} nanowires.

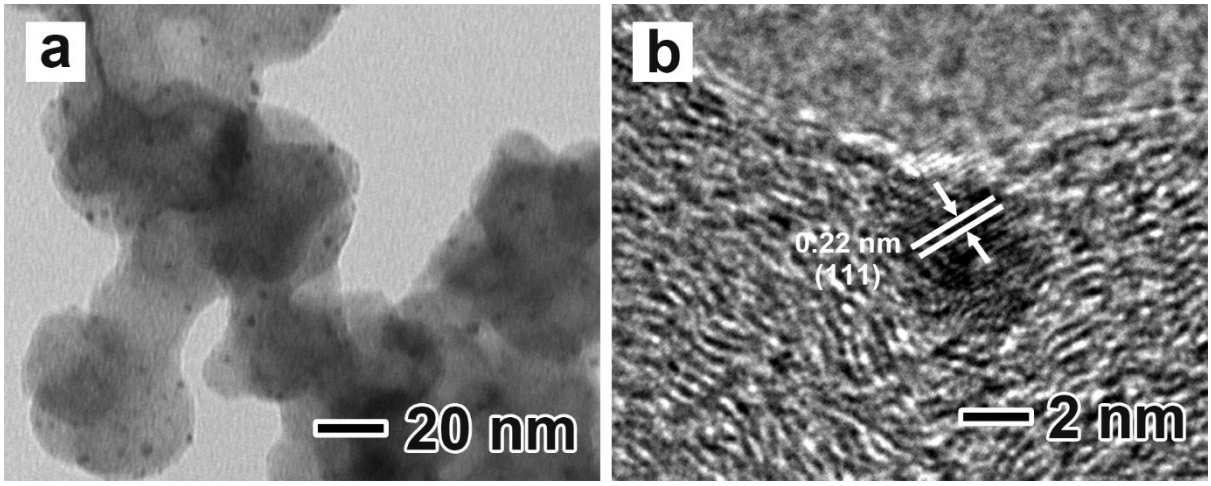

Fig S5. (a) TEM and (b) HRTEM images of the Rh/C catalysts prepared by dispersing the Rh nanoparticles on carbon black supports.

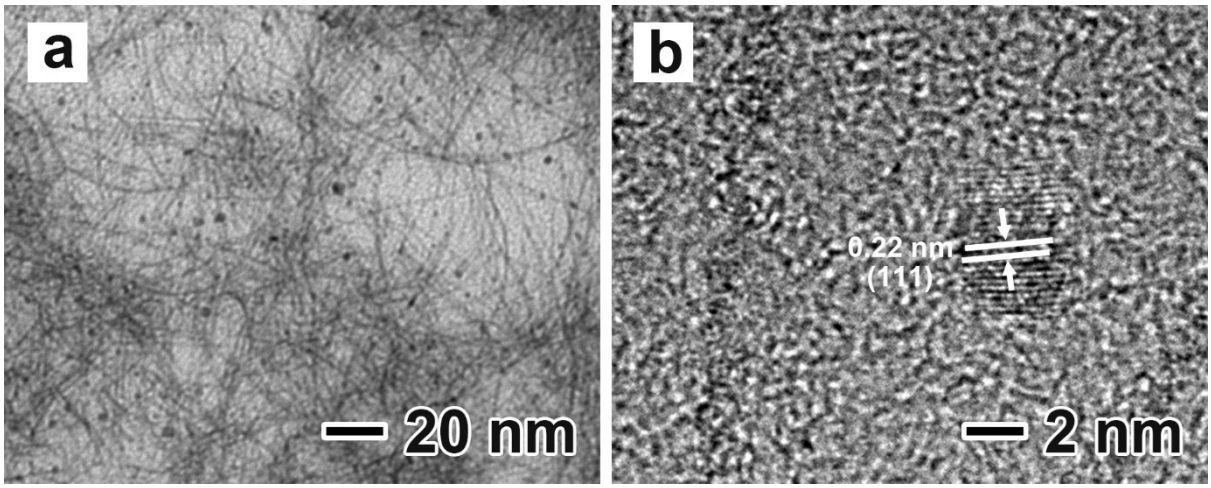

Fig S6. (a) TEM and (b) HRTEM images of the mixed Rh nanoparticles and WO_{3-x} nanowires (Rh+WO_{3-x}).

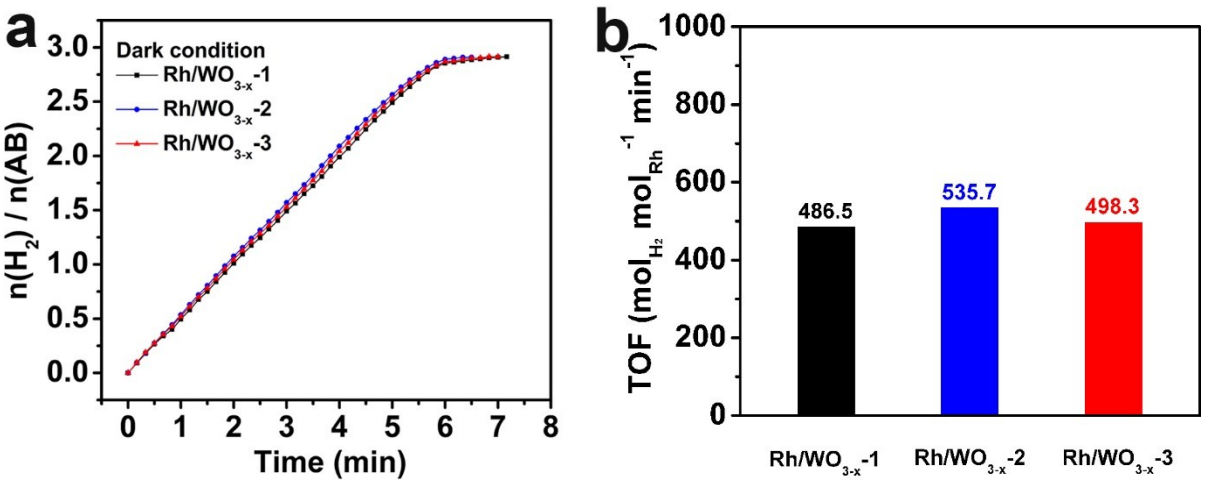

Fig S7. (a) Time courses for hydrogen production from AB over Rh/WO_{3-x}-1, Rh/WO_{3-x}-2, and Rh/WO_{3-x}-3 catalysts and (b) their corresponding TOF values under dark condition.

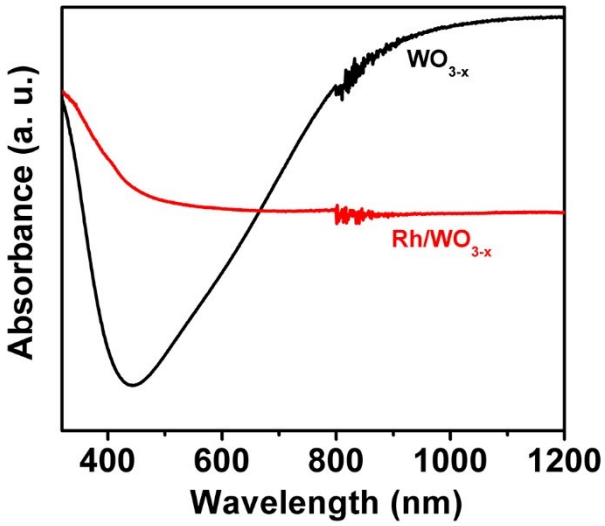

Fig S8. UV-Vis-NIR absorption spectra of Rh/WO_{3-x} hybrid nanowires and WO_{3-x} nanowires.

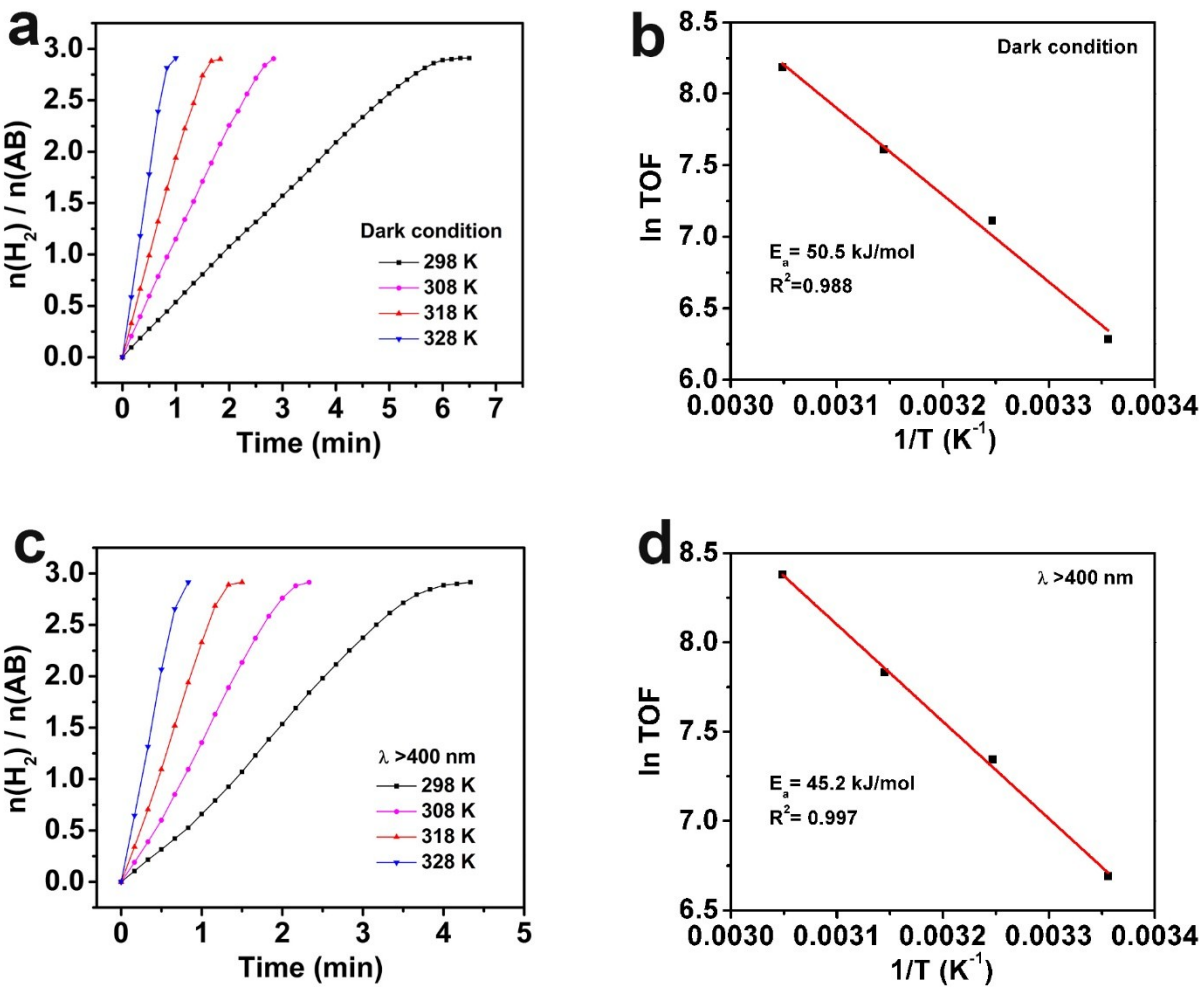

Fig S9. Plots of time versus volume of hydrogen generated from the hydrolysis of AB catalyzed by Rh/WO_{3-x} and corresponding Arrhenius plots under (a, b) dark condition and (c, d) visible light irradiation at different temperatures in the range of 298–328 K, respectively.

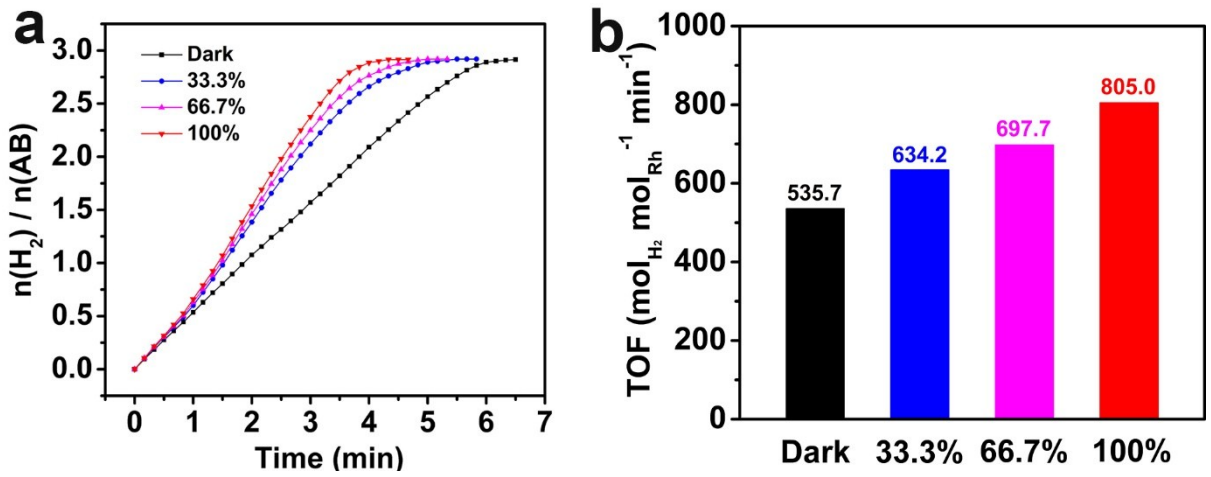

Fig S10. (a) Plots of time versus volume of hydrogen generated from the hydrolysis of AB catalyzed by Rh/WO_{3-x} and (b) the corresponding TOF values under visible light irradiation with di□erent powers of Xe lamp.

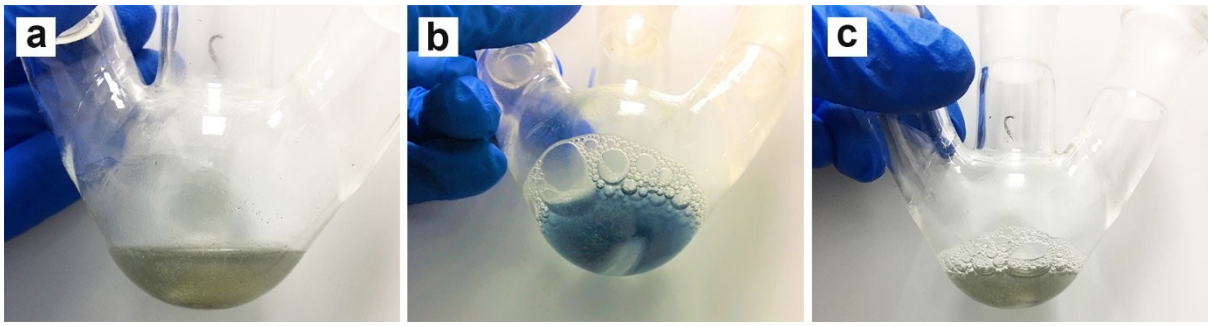

Fig S11. Digital photograph of Rh/WO_{3-x} suspension under different conditions: (a) before catalytic reaction, (b) after catalytic reaction and the flask was kept sealed, (c) after catalytic reaction and the flask was exposed to the air for a little while.

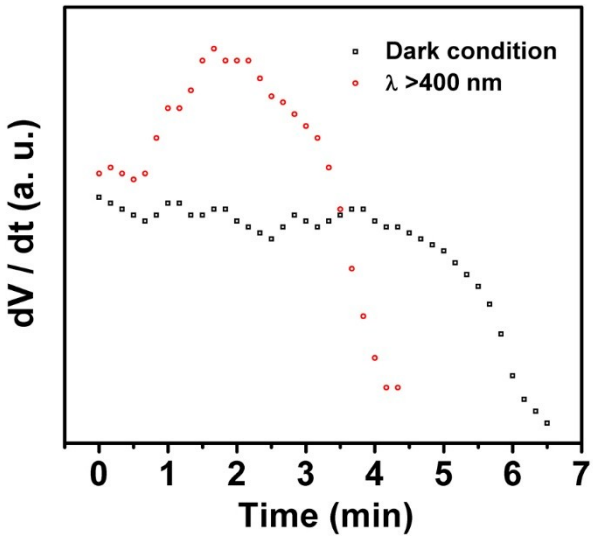

Fig S12. Plots of dV/dt *vs.* t by using Rh/WO_{3-x} as the catalysts under dark condition and visible light irradiation, respectively. The dV/dt is the differential of H_2 production volume (V) to H_2 generation time (t).

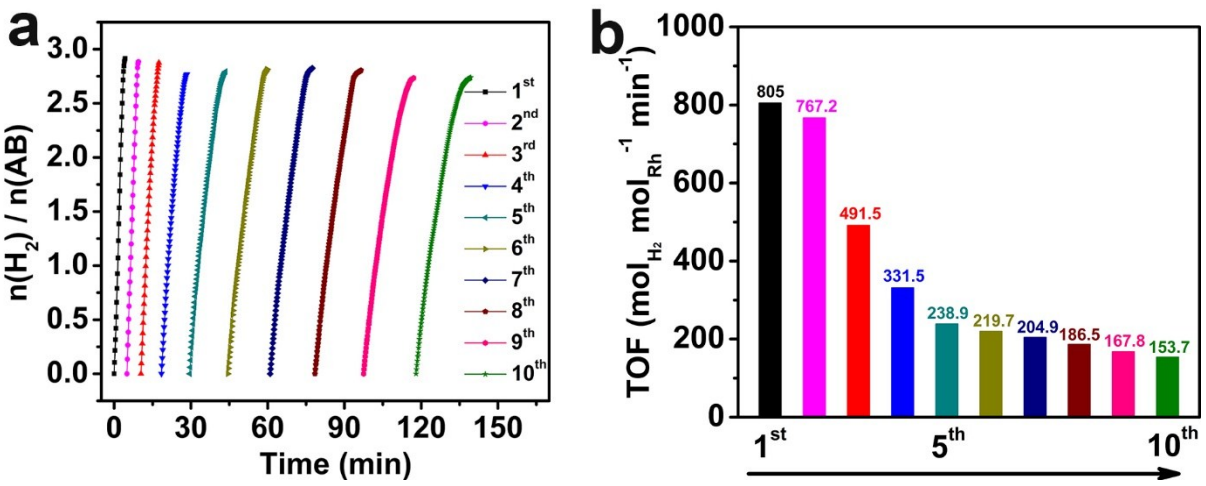

Fig S13. (a) Plots of time versus volume of hydrogen generated from the hydrolysis of AB catalyzed by Rh/WO_{3-x} for ten cycles and (b) the corresponding TOF values.

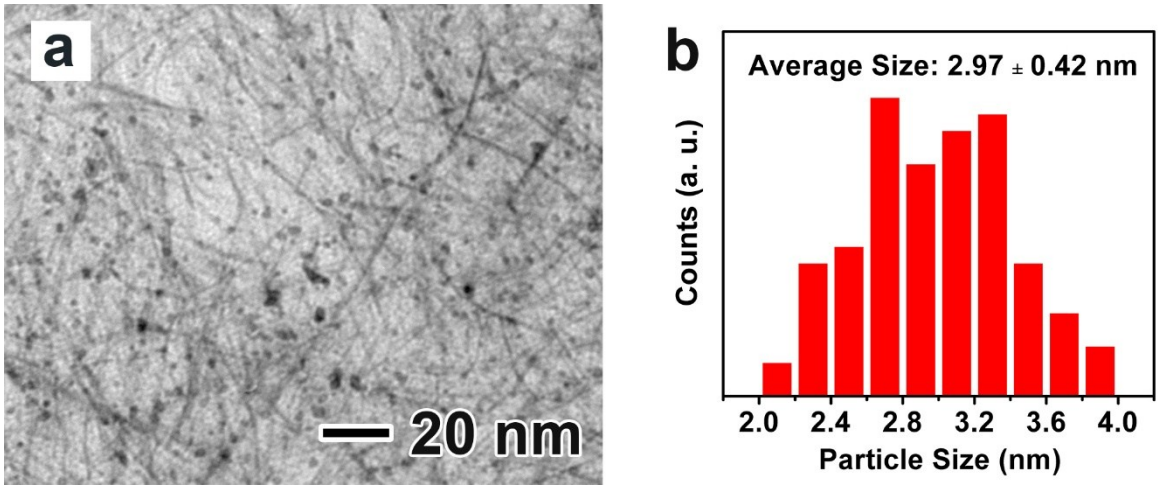

Fig S14. (a) TEM image and (b) size distribution of Rh nanoparticles of the Rh/WO_{3-x} catalysts after the fifth cycle.

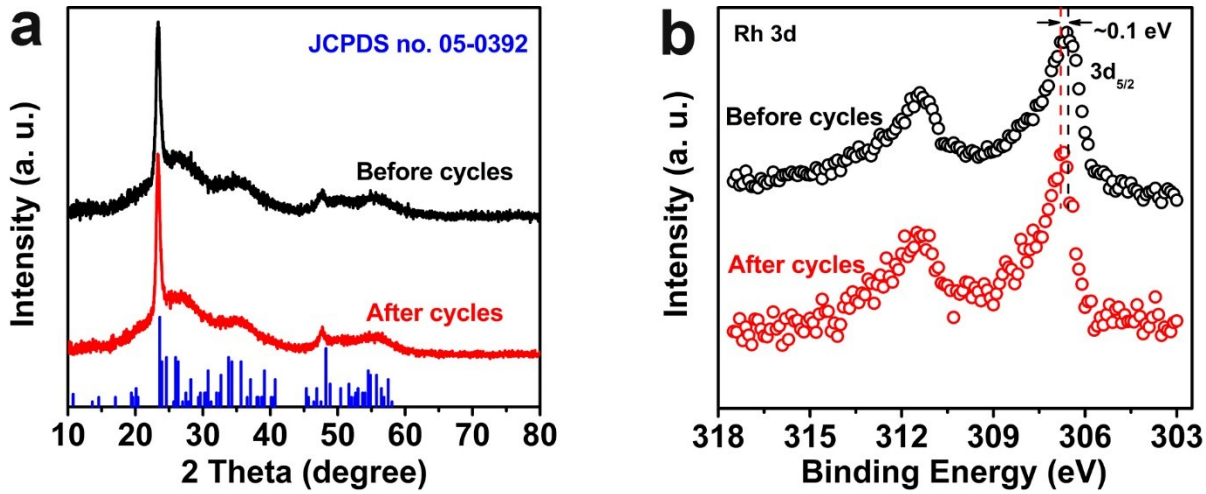

Fig S15. (a) XRD patterns and (b) XPS spectra for Rh 3*d* orbitals of the Rh/WO_{3-x} catalysts before and after the fifth cycle.